BioCore
Exploring Scientific Community

International Journal of Nanotechnology in Medicine & Engineering

Volume 6 Issue 1,
January 2021

Citation

Islam M. I. Moustafa et al. (2021), Superparamagnetic Nano α-Fe2O3 and TiO2 as Photocatalysts and Adsorbents in Wastewater Treatment; Evaluation of Photocatalytic Activity and Biological Response. Int J Nano Med & Eng. 5:1, 01-09

ISSN 2474-8811

Published by
Biocore Group|
www.biocoreopen.org/ijnme/archive.php

Research Article

Superparamagnetic Nano α-Fe2O3 and TiO2 as Photocatalysts and Adsorbents in Wastewater Treatment; Evaluation of Photocatalytic Activity and Biological Response

Islam M. I. Moustafa*, El – Sayed M. Mabrouk, Heba S. Mahfouz

Chemistry Department, Faculty of Science, Benha University, Benha Egypt

Corresponding author: Islam M. I. Moustafa
Chemistry Department, Faculty of Science, Benha University, Benha Egypt.
E-mail: Islamshahin84@outlook.com

Article History: **Received:** January 22, 2021;
Accepted: February 02, 2021;
Published: February xxxx, 2021.

Abstract

Two types of nanosized oxides (Fe2O3 and TiO2) were prepared by simple and ecofriendly method. The as-prepared nano oxides were characterized by Thermogravimetric analysis, FTIR, XRD and HRTEM. As applications, the nano Fe2O3 was tested as photo catalyst for the decontamination of methylene blue (MB) as organic pollutant and the efficiency of TiO2 for the removal of Zn (II) and Pb (II) from water sample were extensively studied. The different factors (time, pH, initial concentration of pollutants and dose of sorbent), sorption mechanism and kinetics of the removal process were studied. The antimicrobial activities of the nano oxides were tested against two of Gram – positive bacteria (Streptococcus pyogenes and Staphylococcus epidermidis) and two Gram – negative bacteria (Proteus vulgaris and Klebsiella pneumonia). Standard drug; levofloxacin and DMF solvent control were screened separately for their antibacterial activity. The antibacterial results showed that the as prepared nanooxides exhibit high activity against the tested organisms. The activity is in the order TiO2 > Fe2O3.

Keywords

Fe2O3, TiO2 nanoparticles, wastewater treatment, methylene blue, metal ion removal, biological activity

Declaration of Conflicting Interest

The author(s) declared no potential conflicts of interest with respect to the research, authorship, and/or publication of this article.

Introduction

Nanostructured materials with unique physical and chemical properties are useful in many fields of live times. Iron oxide nanostructures constitute a very important class of such materials used in a variety of fields, including catalytic applications [1-6]. From the industrial point of view, the main advantages are that the materials are prepared in a nontoxic and economical way and have different crystalline structures that possess unique properties [6]. Iron oxide nanoparticles (NPs) are the most popular magnetic NPs used in biomedical applications, due to their low cost, low toxicity, and unique magnetic properties [7,8]. It has been used in the cosmetic industry, as well as TiO2, ZrO2, ZnO and CeO2 which can act as sun protection factors or pigments in cosmetic products [7]. Nano TiO2 is an efficient photocatalyst and has attracted much attention with the increasing environmental problems because of its stable chemical properties, non-toxic character and no secondary pollution [9]. Nano oxides exhibit great potential in the field of life sciences, such as biomedicine, agriculture, and environmental remediation [10, 11].The decomposition/degradation of organic dyes has been studied extensively in the literature, using visible light in the catalytic process. Nanostructured materials with unique physical and chemical properties are useful for the detection of pesticides, especially in surface and ground water [12]. These NPs are also promising tools for strategies for the elimination and degradation of pesticides in order to remedy environmental pollution in different areas [13]. In this article, and in continuation to our previous work [14], nanosized Fe2O3 and TiO2 were prepared by ecofriendly method and characterized by different techniques. As applications, the Fe2O3 was tested as photo catalyst for the decontamination of MB and the efficiency of TiO2 for the removal of Zn (II) and Pb (II) from water sample. Their antimicrobial activity towards some bacteria was also studied where it was found that they exhibit high activity against the tested organisms. The activity is in the order TiO2 > Fe2O3.

Experimental

All chemicals used in the present study were of the highest quality (Merck, Aldrich or Fluka) and were used without further purification. Freshly bidistilled water was used whenever water is necessary.

Synthesis of Fe2O3 Nanoparticles

The hematite particles were prepared by a hydrothermal treatment of iron (III) nitrate with citric acid according to the following scheme [15]:

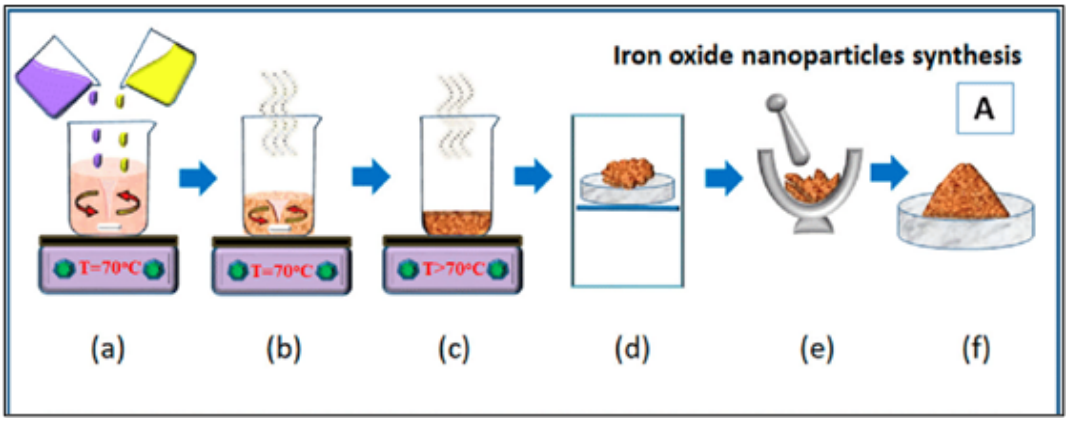

(a) Drop wise mixing of iron nitrate and hydrated citric acid solution at 70°C.
(b) Formation of Iron oxide gel. (c) Drying to remove solution. (d) Annealing of the produced product.
(e) Grinding of the obtained product. (f) Synthesized Fe2O3 nanoparticles.

Synthesis of TiO2 Nanoparticles

Synthesis of TiO2 nanoparticle was carried out according to the simple method described by Lusvardi et.al [16]. In a typical experiment, 50 mL ethanol and 5.0 mL titanium tetrachloride (99 %) were mixed and stirred for 30 min where a yellow sol phase is formed. Bidistilled water was added (200 mL) and the solution became clear and colorless. The solution was again stirred for 30 min at room temperature and then the formed gel was dried at 50 °C for 24 h.

Instruments and characterization methods

Characterization methods and instruments used for structure confirmation were typically as described in our previous work [14].

Antimicrobial screening

The antimicrobial activities of Fe2O3 and TiO2 nano particles were tested against two of Gram – positive bacteria (Streptococcus pyogenes and Staphylococcus epidermidis) and two Gram – negative bacteria (Proteus vulgaris and Klebsiella pneumonia). Standard drug; levofloxacin and DMF solvent control were screened separately for their antibacterial activity. The test was done by the disk diffusion

technique developed by Bauer et al [17] and described in our previous work [18]. The method is based on the determination of an inhibited zone proportional to the bacterial susceptibility to the antimicrobial present in the disk. Three replicas were made for each treatment to minimize error.

The photocatalytic degradation

The photocatalytic activity was evaluated by the decomposition of methylene blue (MB) in aqueous solutions using Fe2O3 nano particle as catalyst. In batch experiment:

- 100 mL of MB dye solution (50 ppm) was added to 20 mg of the catalyst in 250 ml beaker, the solution was kept at 25 ± 0.1oC and at pH = 7.0.
- The solution was stirred at 150 rpm for 30 min to get equilibrium then centrifugate to separate clear solution.
- The absorbance of the resulted solution was measured at 660 nm using spectronic 21 Bauch & Lomb single beam spectrometer
- This experiment was repeated without using catalyst but the solution was irradiated by UV lamp for 30 min.

The experiment was repeated using 100 ml MB dye solution of different concentrations (30, 50, 70 and 100 ppm), different pH's (3.0, 5.0, 7.0 and 10.0) and different temperatures (303, 308 and 313 k) keeping all other parameters constant.

During the experiments the concentration of the dye was determined using a UV-visible spectrophotometer at its maximum wavelength (660 nm).The percent photodegradation efficiency (%Removal) was calculated as:

$$\% \text{ Removal} = (Co-Ct)/Co \times 100 \approx (Ao-At)/Ao \times 100$$

where Co is the initial concentration of the dye solution and Ct is its concentration at time (t). A0 is the absorbance at time t = 0 min and At is the absorbance after t time of treatment. A0 and At are the absorbance recorded at λmax of the dye

Kinetic procedure

The kinetic of the removal process was applied using the pseudo-first-order and pseudo-second-order equations (1 and 2, respectively) [19, 20]:

$$\ln (qe - qt) = \ln qe - k1t \quad (1)$$

where k1 (min−1) is the rate constant of pseudo-first-order adsorption, qt is the amount of dye adsorbed at time t (min), and qe is the amount adsorbed at equilibrium, both in mg/g.

$$t/qt = 1/k2qe2 + t/qe, \quad (2)$$

where k2 (g/(mg min) is the rate constant of pseudo-second order. The parameters of pseudo-first-order (qe and k1) and pseudo-second-order (qe and k2) values for Eqs. 1 and 2 can be considered from the slopes and intercepts of the linear plots of log (qe – qt) against t and t/qt versus t, respectively.

Modified Weber and Morris equation was used to measure the intra-particle diffusion [21]:

$$qt = kdift0.5 + c \quad (3)$$

where qt is the adsorption capacity at any time t and kdif is the intra-particle diffusion rate constant (mg/g min½) and C is the film thickness. Kdif and C values were designed from the slope and intercept of plots of qt versus t0.5, respectively.

Calculation of the thermodynamic activation parameters

Enthalpy of activation, ΔH*, and entropy of activation ΔS*, were calculated using transition state theory equation (Eyring Equation).

$$k = (KT)/h \exp(\Delta S^*/R) \exp(-\Delta H^*/RT)$$

where : K is the Boltzman constant, h is the Plank's constant, R is the universal gas constant, and T is the absolute temperature. Taking the natural logarithms

$$\ln k/T = \ln(K/h) + \Delta S^*/R - H^*/RT$$

A plot of ln (k / T) against 1 / T is linear, with a slope equal (- ΔH* / R) and intercept (ln K / h + ΔS* / R). Therefore, ΔH* and ΔS*can be calculated from the slope and intercept, respectively.

Removal of heavy metals [Zn (II) and Pb (II)]

The efficiency of the as-prepared TiO2 NP's for the removal of Pb2+ and Zn2+ metal ions from water samples was assessed. For the preparation of synthetic wastewater, stock metal ion solutions (1000 mg/l) were prepared by dissolving 4.978 g Pb(NO3)2.H2O, and 4.396 g ZnSO4.7H2O in 1000 ml double-distilled water. All working solutions of different concentrations were prepared by diluting the stock solution with distilled water. The pH of the test solutions was adjusted using reagent grade dilute hydrochloric acid and sodium hydroxide (0.1M). InoLab 726 pH meter (Ser-No 09210173) was used to measure the pH of solutions. The metal ion concentrations were measured by atomic absorption spectrometer (Szhimadzu AA7000) (Faculty of Agriculture, Benha University, Egypt).

Investigated parameters:

The effect of contact time (5 – 120 minutes), adsorbent dos (0.02 – 0.12 g/l), pH (2.0, 3.5, 5.5, and 7), initial concentrations of metal ion (20, 50, 75, 100 and 120 ppm) on the removal efficiency of metal ion was processed keeping all other parameters constant.

Results and Discussion

Characterization of the nano oxides

1. Thermogravimertic analysis(TGA)

The thermogravimeteric – differential thermal analysis shows that Fe2O3 NP exhibits no thermal events up to 749.34oC where a weak endothermic peak was obtained with a corresponding weight loss of 5.63%. This is due to the transformation of Fe2O3 (initially formed) to Fe3O4 according to the equation:

$$6Fe2O3 \rightarrow 4\ Fe3O4 + O2$$

TiO2 thermogram shows degradation in two stages; the first is very weak corresponding to elimination of humidity water while the second (with 4.5% Wt. Loss) is due to removal of coordinated water molecules. After this step, TiO2 shows higher resistance to thermal degradation up to about 800oC

2. Fourier Transform infrared spectra (FTIR)

As expected, the IR spectra of Fe2O3 and TiO2 exhibited the characteri k= (KT)/h exp(ΔS^*/R) ex p(-ΔH^*/RT) stic absorption bands in the short wave region around 600 and 690 cm–1 respectively, due to νM-O stretching frequencies. The spectrum of TiO2 (Fig. 1) showed weak broad band at 3454 cm-1 which is due to stretching hydroxyl (O-H), representing the water as moisture. The other peak at 1631 cm-1 is due to stretching of titanium carboxilate, which formed from ethanol as precursors. The shift in the IR active mode is due to nano size grain. For a nano sized grain, the atomic arrangement on the boundaries differs greatly from that of the bulk crystals, both in coordination number and bond lengths, showing some extent of disorder [22]. Crystal symmetry is thus, degraded in nano size grains.

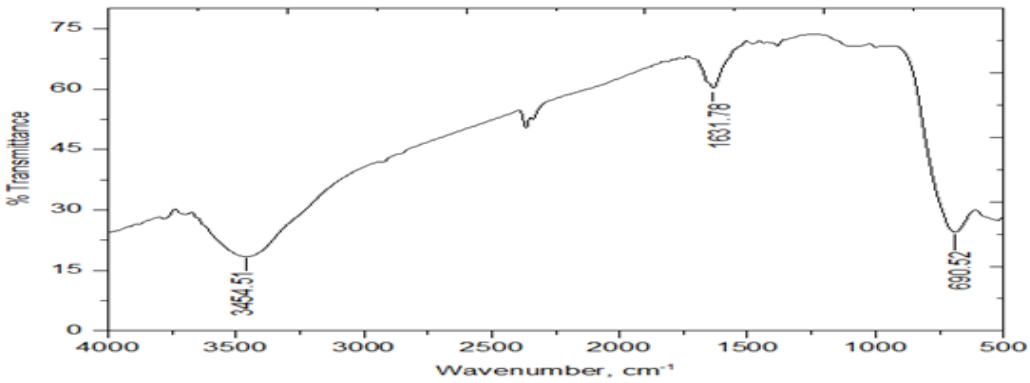

Fig 1 IR spectrum of TiO2 nano particle

3. X-Ray diffraction analysis (XRD)

The XRD pattern of Fe_2O_3 nanoparticle, confirms the formation of Fe_2O_3 phase in the sample. The average particle size of the nanoparticle determined by using the Scherrer equation was found to be 35.4 nm. The peaks were matched using JCPDS software and it was well matched with the Fe_2O_3 of file no "Pdf # 892810".

The phase composition and the crystallite size of the prepared TiO_2 sample were evaluated by X-ray diffraction analysis. The peaks of sample were identified by comparison with JCPDS-84-1286 according 2θ which confirmed an anatase structure at 20=25.4o. From calculation, the average crystalline size was found to be 21.7 nm. The samples show very thin peaks, indicating the fine nature and small crystallite size of the particles.

4. High Resolution Transmission Electron Microscopy (HRTEM)

The morphology of the as synthesized samples were investigated using HRTEM. The TEM images showed that Fe_2O_3 nanoparticles have narrow size distribution and are rectangular rode shapes with weak agglomeration. The average particle sizes ranged from 22.49 to 44.45 nm. While that of the TiO_2 nanoparticles (Fig. 2) showed that almost all of the particles have spherical shape and the results are in good agreement with XRD data measured using Scherrer's equation.

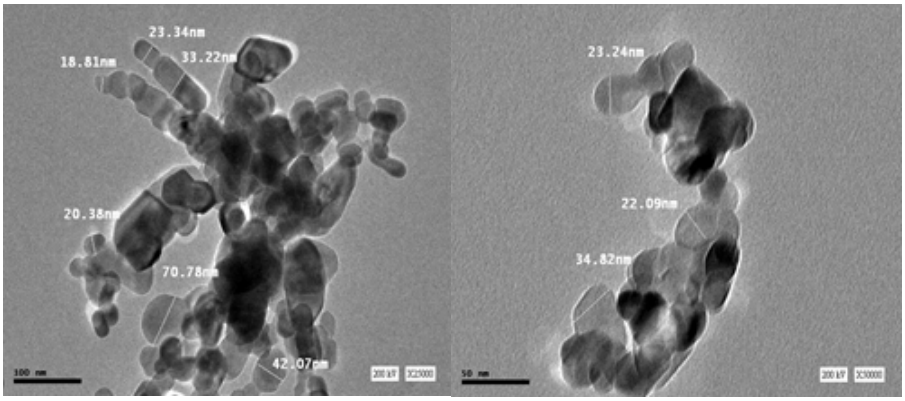

Fig 2 HRTEM for TiO2 nano particle with different magnification power

Analytical application

1. Photocatalytic activity of Fe2O3

The photocatalytic activity was evaluated by the decomposition of methylene blue (MB) in aqueous solutions using Fe_2O_3 nano particle as catalyst. The percent degradation efficiency was studied by photoirradiation only and by using Fe_2O_3 as catalyst. It was found that photoirradiation of the dye without catalyst showed low degradation efficiency with maximum efficiency of about 50% after 80 min while removal reached about 85% on using Fe_2O_3 as catalyst within the same time. The following factors were extensively studied:

Effect of primary dye concentration

The effect of primary concentration of MB dye (30, 50, 70 and 100 ppm) in the presence of Fe_2O_3 as catalyst was studied. The results are illustrated graphically in Fig. (3). It is clear from the figure that there is an increase in the percentage removal of MB by decreasing its concentrations. The uptake of MB by Fe_2O_3 for 30 ppm of dye concentration reached to about 100% after 100 min while that for 100 ppm is 62.5% within the same time. These results are due to the saturation of adsorption sites on the surface of adsorbent.

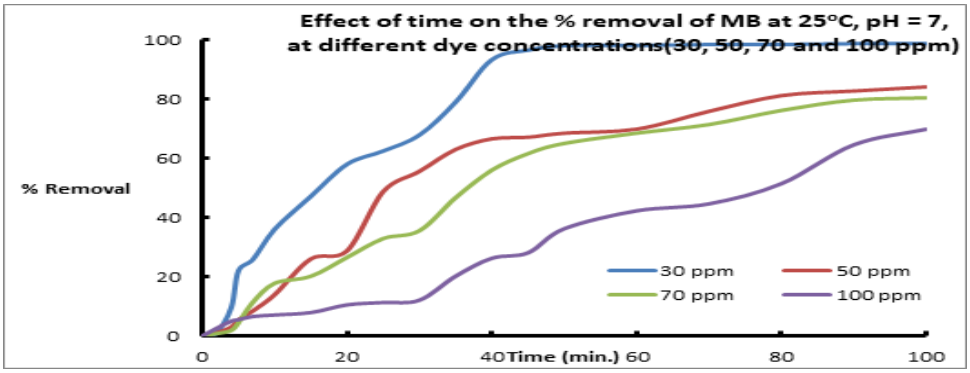

Fig 3 Effect of time on the % removal of MB using Fe2O3 as catalyst

Effect of solution pH

The removal of MB on Fe_2O_3 was studied in different pH range of (3–10). The result represented in Fig. (4) shows that the percentage of dye removal decreases by increasing the pH value from 3.0 to 5.0 but, when the pH is increased to 8.0, the maximum adsorption increased and further decrease occurred in removal with increasing pH value to ≥ 10.

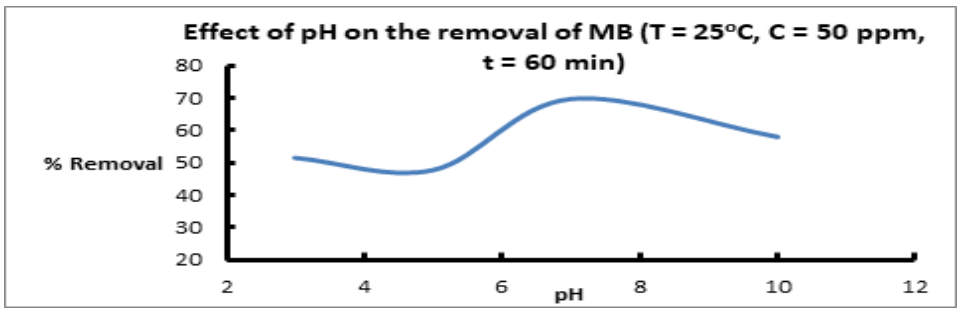

Fig 4 Effect of pH on the % removal of MB using Fe2O3 as catalyst

It is known that, as the pH increases, the amount of sites have positive charged decreases and the number of sites have negative charged increases. Applying dye adsorption over pH = 8.2, the surface becomes negatively charged due to the presence of functional group such as OH– group, MB cationic dye adsorption is more preferable. In the same way, the decrease in adsorption of MB cationic dye molecules happens at low pH < 7 because of electrostatic repulsive. Therefore, the optimum pH for higher MB removal from aqueous solution is 7 - 10.

Effect of temperature

The effect of temperature on the rate of removal of MB dy was studied over the temperature range 25 – 35oC. It was found that as the temperature increase, the percent rate of degradation increases. The rate constants of the dye removal at different temperatures were calculated using the relations:

$$\ln[A]_{(t)} = \ln[A]_{(0)} - kt$$

From which a plot of (lnAt) against time (t), (c.f. Fig.5) yields a straight line from which the rate constant k can be obtained.

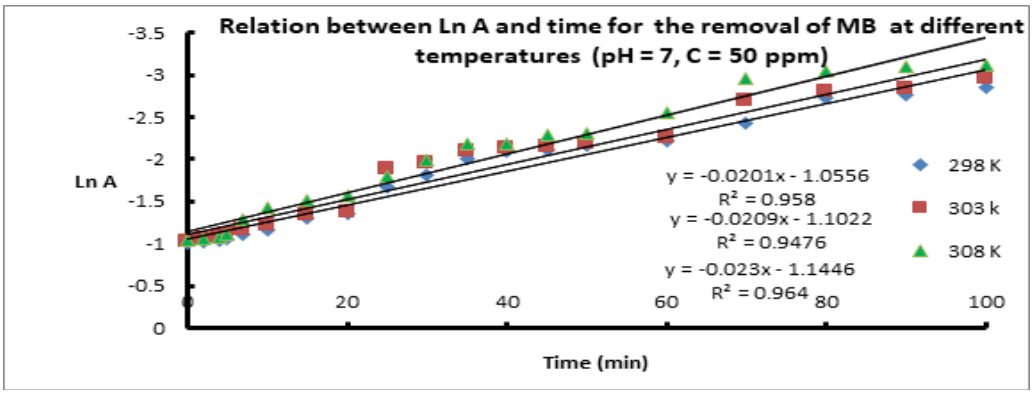

Fig 5: Relation between ln A and Time for the removal of MB using Fe2O3 as a catalyst at different temperatures.

Calculation of the thermodynamic activation parameters

Enthalpy of activation, ΔH*, and entropy of activation ΔS*, were calculated using transition state theory equation

(Eyring Equation) in logarithmic form:

$$\ln k/T = \ln(K/h) + \Delta S^{*}/R - \Delta H^{*}/RT$$

where : K is the Boltzman constant, h is the Plank's constant, R is the universal gas constant, and T is the absolute temperature. A plot of ln (k / T) against 1 / T is linear (Fig. 6), with a slope equal (- ΔH* / R) and intercept

(ln K/h+ΔS*/R). Therefore, ΔH* and ΔS*can be calculated from the slope and intercept, respectively. The thermodynamic parameter; free energy change of activation ΔG* is calculated using the equation:

$$\Delta G^{*} = \Delta H^{*} - T\Delta S^{*}$$

The thermodynamic activation parameters were calculated and listed in Table(1). The data listed in Table (1) revealed that ΔH* has positive value indicating that the degradation of the dye is indothermic process. Also, the negative values of ΔS* revealed that the activated complex in the rate determining step represents an association rather than dissociation which means that a decrease in disordering takes place on going from reactants to the activated complex. Also, the negative sign of ΔG* reflect that the degradation of the dye in the activated complex is spontaneous process.

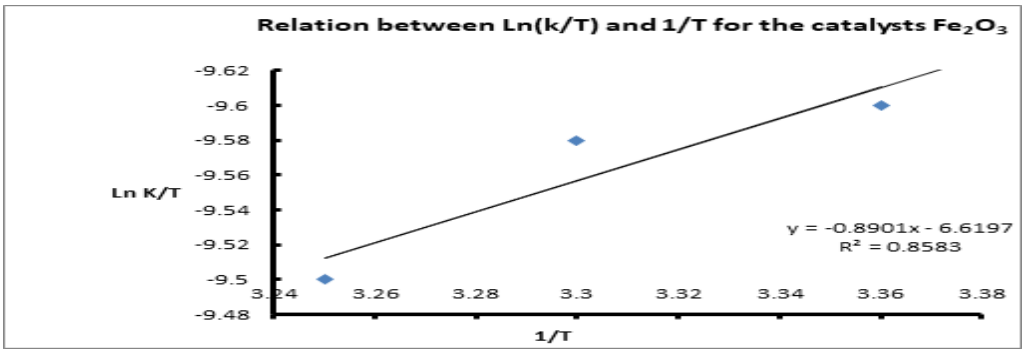

Fig 6 Relation between Ln(k/T) and 1/T for the catalysts Fe2O3

Sorption kinetic modeling

Pseudo – first order and pseudo – second order rate equations were applied to analyze the adsorption kinetics of MB from wastewater onto NPs surface at 25±1oC. The linearized forms of the pseudo 1st order and the pseudo – second order model are given by:

$$\log(q_e - q_t) = \log q_e - k_1/2.303\ t \quad (1)$$

$$t/q_t = 1/(k_2 q_e^2) + 1/q_e\ (t) \quad (2)$$

The parameters of pseudo-first-order (qe and k1) and pseudo-second-order (qe and k2) values for equations 1 and 2 can be obtained from the slopes and intercepts of the linear plots of Ln (qe – qt) against t and t/qt versus t, respectively. The sorption kinetic data are cited in Table (1) from which it is clear that the pseudo first order model is the better applicable.

Modified Weber and Morris equation was used to measure the intra-particle diffusion [23]:

$$q_t = k_{dif}\, t^{0.5} + c \quad (3)$$

where qt is the adsorption capacity at any time t and kdif is the intra-particle diffusion rate constant (mg/g min½) and C is the film thickness. Kdif and C values were calculated from the slope and intercept of plots of qt versus t0.5, respectively (Table 1). Applying intraparticle diffusion model showed that the adsorption process displays multi-linear plot. The value of kdif obtained from the slope of linear plots (Fig. 7) is 5.5172 (mg/min½ g). The plot does not pass through the origin therefore, the rate determining in the dyes adsorption process might be the boundary layer (film) diffusion.

Thermodynamic parameters			Pseudo 1st order		Pseudo 2nd order		Weber and Morris constants	
ΔH*	ΔS*	ΔG*	K1	R2	qe	R2	Kdif.	C
7.400	-271.69	-80.96	0.046	0.9535	1250	0.0015	5.5172	7.2895

Table 1 Thermodynamic, kinetic and Weber and Morris parameters for the removal of MB dye using Fe2O3 as catalyst

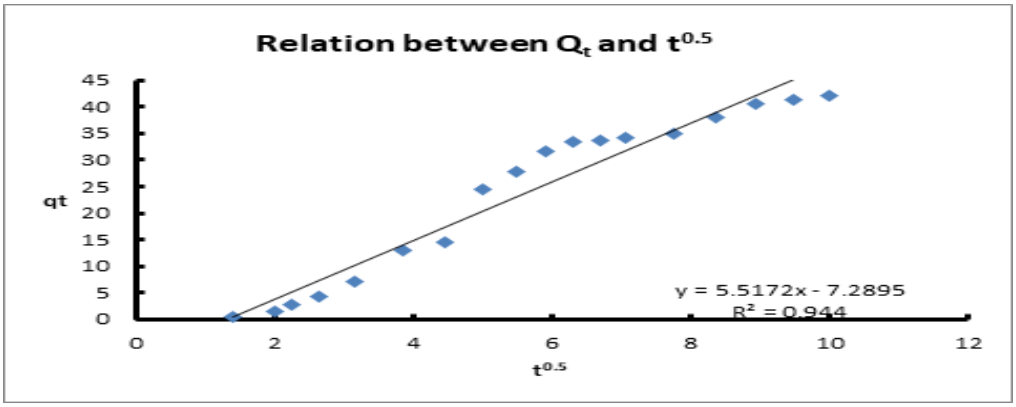

Fig 7 Relation between Qt and $t^{0.5}$

Adsorption isotherms

Two adsorption isotherms (Langmuir, and Freundlich) were used in order to correlate the equilibrium adsorption data. The value of the correlation coefficients R2, has been used as a test criterion for the fit of the correlation.

Langmuir Model

The Langmuir equation is the most widely used two-parameter equation, commonly expressed as

$$C_e/q_e = 1/bQ_o + C_e / Q_o \quad (4)$$

where C_e is the equilibrium concentration of MB remaining in the solution(mgdm^{-3}), q_e is the amount of adsorbate adsorbed per mass unit of adsorbent at equilibrium (mgg^{-1}), Qo and b are Langmuir constants. Langmuir equation can be used to calculate the maximum adsorption Qo (mgg^{-1}) and the energy parameter of adsorption b (dm^3 mg^{-1}) from the slope and intercept of the line, obtained from the plot of C_e/q_e vs C_e (Fig. 8).

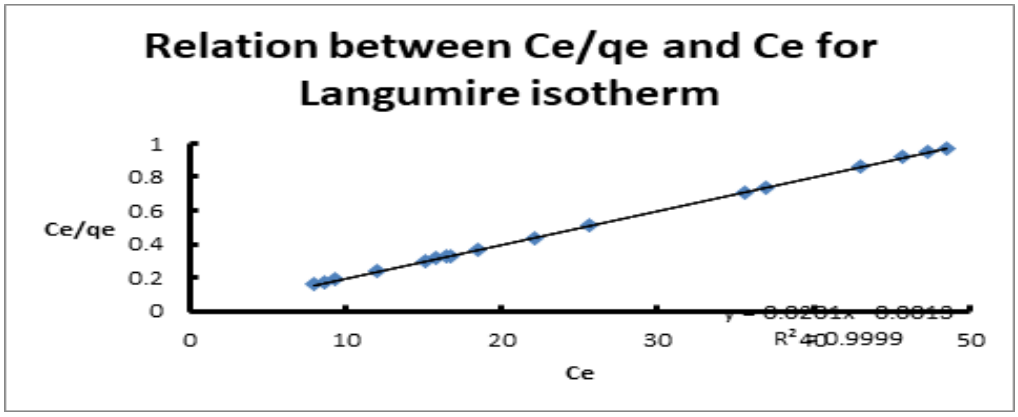

Fig 8 Relation between Ce/qe and Ce for Langumire isotherm

Freundlich model

The Freundlich isotherm assumes that the adsorption occurs on heterogeneous surface at sites with different energy. Its empirical equation has the following linear form:

$$\log q_e = \log k_F + 1/n \log C_e$$

where Ce and qe have the same meaning; K_F and 1/n are constants that are considered to be relatively indicators of adsorption capacity (or related to the bonding energy) and adsorption intensity , respectively. A value for 1/n below one indicates a Langmuir-type isotherm because it becomes more and more difficult to adsorb additional adsorbate molecules at higher adsorbate concentrations. A plot of log q_e vs. log C_e enables the empirical constants k_F and 1/n to be determined from the slope and intercept of the linear regression as shown in Table (2).

Langmuir constants			Freundlich constants		
Qo(mgg-1)	b(dm3g-1)	R2	KF	n	R2
49.75	15.46	0.9999	82.64	0.627	0.765

Table 2 Values of Langmuir and Freundlich constants for the removal of MB using Fe2O3 as catalyst

2. Adsorption of Zn (II) and Pb (II):

The efficiency of the as-prepared TiO2 nanooxide for the removal of Zn(II) and Pb(II) from water samples was assessed. The effect of different parameters controlling the removal process was studied. The following parameters were studied

Effect of initial concentration:

The effect of initial metal concentrations ranging 20 – 120 ppm was studied. The equilibrium data revealed that, percent adsorption increased with increase in initial metal ions concentration up to 80 ppm. This means that the adsorption is highly dependent on initial concentration of metal ion. It is because of that at lower concentration, the ratio of the initial number of metal ion to the available surface area is low subsequently the fractional adsorption becomes independent of initial concentration. However, at high concentration the available sites of adsorption becomes fewer and hence the percentage removal of metal ion is dependent upon initial concentration.

Effect of contact time:

Results indicate that removal efficiency increased with an increase in contact time before equilibrium is reached. Other parameters such as dose of sorbent, pH of solution and initial concentration was kept constant, while temperature was kept at 25ºC. This result is important, as equilibrium time is one of the important parameters for an economical wastewater treatment system. The study indicated that maximum equilibrium takes place after 100 min

Effect of pH:

pH is an important parameter for adsorption of metal ions from aqueous solution because it affects the solubility of the metal ions and the degree of ionization. To examine the effect of pH on the Zn2+ and Pb2+removal efficiency, the pH was varied from 2.0 to 8.0 as shown in Fig. (9). The data showed that at lower pH value there is lower % removal of both metal ions that is simply due to the plenty of H+ which compete with the metal cation. At pH value higher than 3.0, considerable jump in the percent removal is observed to reach about 65 – 70 %. Further increase in the pH value led to precipitation of metal ion and separation from solution. So, the optimum pH for removal of both metal ions is at the interval between

5.0 and 6.0. It is known that metal ion species [M(II)] present in aqueous media in the form of M^{2+}(aq) and $M(OH)_2$(S). At high pH, the precipitation of M(OH)2(S) plays an important role in removing the metal ion. So, the sorption process should be done at pH< pH of precipitation. Theoretical value for precipitation of Pb^{2+} and Zn^{2+} as hydroxides can be calculated from the knowledge of their solubility products of $Pb(OH)_2$ (1.2x10-15) and Zn(OH)2(3.0x10-17) found to be 9.12 and 8.17 for Pb^{2+} and Zn^{2+} respectively.

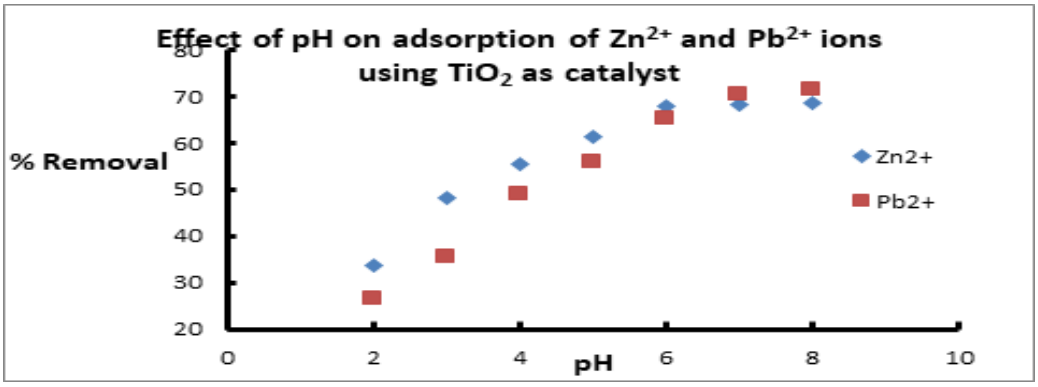

Figure 9 Effect of pH on adsorption of Zn2+ and Pb2+ ions using TiO2 as catalyst

Effect of dose

The dependence of Zn^{2+} and Pb^{2+} sorption on dose was studied by varying the amount of sorbent dose from 20 to 140 mg, while keeping other parameters (pH, initial concentration, and contact time) constant. From results, it can be seen that removal efficiency generally improved with increasing dose and reached maxima at 120 mg. This is expected due to the fact that the higher dose of adsorbents in the solution, the greater availability of exchangeable sites for the ions.

From the preceding studies, the optimum conditions for removal of Pb^{2+} and Zn^{2+} from polluted water can be summarized as given in Table3.

Parameter	Pb2+	Zn2+
Initial meta ion concentration	80 ppm	70 ppm
Time (min)	100	80
pH	5.0	5.0
Sorbent dose (mg)	100	80
Temperature	25°C	25°C

Table 3 Optimum parameters for the removal of Pb^{2+} and Zn^{2+} from polluted water

Antimicrobial activity

The antimicrobial activities of Fe_2O_3 and TiO_2 nano particles were tested against two of Gram – positive bacteria (Streptococcus pyogenes and Staphylococcus epidermidis) and two Gram – negative bacteria (Proteus vulgaris and Klebsiella pneumonia). Standard drug; levofloxacin and DMF solvent control were screened separately for their antibacterial activity. The antibacterial results are listed in Table 4 which suggest that the as prepared nanooxides show high activity against the tested organisms. The activity is in the order TiO_2 > Fe_2O_3. The positive results are due to the diffusion of the nano particles into the lipid layer of the cell membrane of bacteria making them able to kill the bacterium as indicated by the zones of inhibition of bacterial growth.

Organism	Strept. Pyog			Staph. Epid.			Prot. Vulgaris			Kleb. Pne.		
Conc. (µg/mL)	5	10	20	5	10	20	5	10	20	5	10	20
Levofloxacine	12	16	22	15	18	25	12	15	25	15	18	25
Fe2O3	10	13	20	14	14	19	10	13	20	11	20	27
TiO¬2	12	14	22	16	14	21	12	13	23	13	14	20

Table 4 Inhibition zone diameter (mm) of the Fe2O3 and TiO2 against the studied microorganisms relative levofloxacin drug

References

[1] [M. Rincón Joya, J. B. Ortega, J. O. Malafatti and E. C. Paris " Evaluation of Photocatalytic Activity in Water Pollutants and Cytotoxic Response of α-Fe2O3 Nanoparticles ; ACS Omega, 4, (17), (2019), 17477–17486

[2] J. Liu, H. Yang, X. Xue "Preparation of different shaped α–Fe2O3 nanoparticles with large particle of iron oxide red" Cryst. Eng. Comm , 21, (2019), 1097– 1101, DOI: 10.1039/c8ce01920g

[3] K. Vikrant, D. C. W. Tsang, N. Raza, B. S. Giri, D. Kukkar and K. Kim, "Potential Utility of Metal-Organic Framework-Based Platform for Sensing Pesticides" ACS. Appl. Mater. Interfaces, 10,(2018), 8797– 8817, DOI: 10.1021/acsami.8b00664

[4] B. Tsedenbal, I. Hussain, M. S. Anwar and B. H. Koo "Morphological, Magnetic and Optical Properties of α–Fe2O3 Nanoflowers" J. Nanosci. Nanotechnol. ,18, (2018), 6127– 6132, DOI: 10.1166/jnn.2018.15614

[5] K. H. Ng, L. J. Minggu, W. F. Mark-Lee, K. Arifin, K. and M. A. Hafizuddin;"new method for the fabrication of a bilayer WO3/Fe2O3 photoelectrode for enhanced photoelectrochemical performance" Mater. Res. Bull.,98, (2018),47– 52. DOI: 10.1016 / j. materresbull.2017.04.019

[6] D. Lopez-Tejedor, R. Benavente and J. M. Palomo; "Iron nanostructured catalysts: design and applications" Catal. Sci. Technol., 8, (2018), 1754– 1776, DOI: 10.1039/c7cy02259j

[7] A. Akbarzadeh,M. Samiei, and S. Davaran; "Magnetic nanoparticles: preparation, physical properties, and applications in biomedicine" Nanoscale Res.Lett. , 7,(2012), 144, DOI: 10.1186/1556-276x-7-144

[8] W. Wu,Z. Wu,T. Yu, C. Jiang, and W. S. Kim; "Recent progress on magnetic iron oxide nanoparticles: synthesis, surface functional strategies and biomedical applications" Sci. Technol. Adv. Mater. , 16, (2015), 023501, DOI: 10.1088/1468-6996/16/2/023501

[9] W. Chang, M. Zhang, X. Ren and A. Miller; "Synthesis and photocatalytic activity of monolithic Fe2O3/ TiO2" S. Afr. j. Chem. (Online) ,70 (2017)

[10] B. Dabirvaziri, M. H. Givianrad and I. M.H., Sourinejad " A simple and effective synthesis of magnetic γ-Fe2O3@SiO2@TiO2–Ag microspheres as a recyclable photocatalyst; dye degradation and antibacterial potential" J. Environ. Health Sci Engineer, 17, (2019), 949–960. https://doi.org/10.1007/s40201-019-00410-w

[11] V. Nogueira , I. Lopes , T. A. P. Rocha-Santos , F. Gonçalves and R. Pereira;" Treatment of real industrial wastewaters through nano-TiO2 and nano-Fe2O3 photocatalysis: case study of mining and kraft pulp mill effluents" Environ. Technol. 39(12), (2018), 1586-1596. doi: 10.1080/ 09593330. 2017.1334093.

[12] T. S. A. Bhalerao " A review; applications of iron nanomaterials in bioremediation and in detection of pesticide contamination" Int. J. Nanopart. , 7, (2014), 73– 80, DOI: 10.1504/ijnp.2014.062034

[13] A. Rani, R. Reddy, U. Sharma, P. Mukherjee, P. Mishra, A. Kuila and L. C. Sim; " A review on the progress of nanostructure materials for energy harnessing and environmental remediation" J. Nanostruct. Chem. , 8, (2018), 255– 291, DOI: 10.1007/s40097-018-0278

[14] Islam M. I. Moustafa, El-Sayed M. Mabrouk and Mona M. Ashraf; " Photocatalytic removal of organic pollutants from industrial wastewater using MnO, NiO and mixed MnO-NiO NP's as catalyst" Int. j. Nano Med. & Eng, 4(6), 46-55, (2019).

[15] N. Basavegowda, K. Mishra and Y. R. Lee" Synthesis, characterization, and catalytic applications of hematite (α-Fe2O3) nanoparticles as reusable nanocatalyst", Advances in Natural Sciences: Nanoscience and Nanotechnology, 8, (2), (2017),

[16] G. Lusvardi, C. Barani , F. Giubertoni and G. Paganelli" Synthesis and Characterization of TiO2 Nanoparticles for the Reduction of Water Pollutants" Materials 2017, 10, 1208; doi:10.3390/ma10101208

[17] A. W. Bauer, W. M. M. Kirby,J. C. Sherris and M. Turck; Am. J. Clin Pathol 45,(1966), 493–496

[18] A. S. Amin, I. M. I. Moustafa and D. Sh. Saleh," Green synthesis of silver nanoparticles using the extract of mango leaves; biological and cytotoxic effects", Current Topics in Biotechnology, 10, (2019)

[19] H. R. Mahmoud, S. M. Ibrahim, S. A. El-Molla "Textile dye removal from aqueous solutions using cheap MgO

nanomaterials: adsorption kinetics, isotherm studies and thermodynamics" Adv. Powder Technol. 27, 223–231 (2016)

[20] El-Harby, N.F., Ibrahim, S., Mohamed, N.A.: Adsorption of Congo red dye onto antimicrobial terephthaloyl thiourea cross-linked chitosan hydrogels. Water Sci. Technol. 76, 2719–2732 (2017)

[21] Yang, X., Yi, H., Tang, X., Zhao, S., Yang, Z., Ma, Y., Feng, T., Cui, X.: Behaviors and kinetics of toluene adsorption-desorption on activated carbons with varying pore structure. J. Environ. Sci. 67, 104–114 (2018). Exp

[22] J. Yua and D. Kimb; Powder Tech. 235 (2013), 1030-1037.

[23] Yang, X., Yi, H., Tang, X., Zhao, S., Yang, Z., Ma, Y., Feng, T., Cui, X.: Behaviors and kinetics of toluene adsorption-desorption on activated carbons with varying pore structure. J. Environ. Sci. 67, 104–114 (2018)